Chapter 6

IRS-Assisted UWB System

In this Chapter, an IRS-assisted UWB communication system, referred to as IUWB, is studied with the objective of enhancing energy efficiency. To address the limitations of coherent phase shift (CPS) schemes at IRS, a novel strongest-path-based phase optimization method is proposed, leveraging time-resolved UWB multipath characteristics. Analysis encompasses the evaluation of BER and sum-rate performance of IUWB, comparing it against a standard UWB system without IRS.

6.1 Introduction

IRS-assisted communication systems are being studied in the literature to improve the spectral and energy efficiency of the next-generation wireless networks [32, 74, 112, 113]. In IRS-assisted communication, a virtual LoS scenario can be created even in situations where a direct path between the transmitter and receiver is unavailable [32, 114]. IRS comprises multiple independent reflecting elements capable of redirecting incoming signals towards desired directions. Unlike active relays

used in cooperative communications, IRS elements are passive devices without RF chains and advanced signal processing capabilities [115]. By strategically deploying IRS panels in wireless environments and coordinating their reflections, the wireless channels can be dynamically reconfigured to achieve desired distributions at user equipment (UE).

Recently, IRS-assisted wireless systems are explored to enhance energy and spectral efficiency using the passive beamforming at the IRS panel [67, 84, 116, 117]. The IRS includes multiple reflecting elements, which can focus the signal in a particular direction by optimizing the angle of each reflecting element [118]. Further, UWB technology offers several compelling advantages, including ultra-fast data transmission rates, low power consumption, and robustness against interference. It allows for precise and reliable positioning and tracking applications, making it ideal for emerging technologies such as indoor positioning, asset tracking, and sensor networks. In addition, by integrating IRS into UWB systems, it becomes possible to mitigate the challenges posed by signal attenuation, path loss, and interference, especially in complex indoor or urban environments. IRS-assisted UWB communication promises to extend the range, improve coverage, and increase data rates, making it particularly well-suited for applications such as high-speed data transfer, indoor positioning, and industrial IoT (IIoT) connectivity. The IRS-assisted system improves the BER and coverage area of users served for future communication applications with higher energy efficiency in UWB. BER, sum-rate, and outage probability are analyzed for UWB without IRS [48–50]. A supervised learning-based UWB ranging error mitigation [24, 51], UWB channel models [23], and order statistic-based non-coherent UWB receiver [52] are analyzed. Further, IRS-assisted localization system analysis is also considered in literature [53–55]. Additionally, IRS-assisted OMA [119, 120], NOMA [121, 122], and terahertz [123] communication are studied in the literature.

To the best of the authors' knowledge, IRS-assisted UWB systems are not explored in the literature. Therefore, it is interesting to analyze an UWB system with IRS especially for low SNR scenarios[1], and to understand the effect of IRS on various parameters of the UWB system.

We note that, due to ultrawide bandwidth of UWB, the system formulation is different than conventional narrow band systems considered in the literature [124, 125]. For instance, coherent phase setting at the IRS panel is not practically possible in UWB due to multipath. In IRS-assisted UWB, the phase setting is optimized for a wideband system, hence, it is intractable to solve optimally. Thus, the overall system design for IRS-based communication for UWB systems is different and more challenging compared to conventional narrow-band studies.

Contribution : For the first time an IRS-assisted downlink UWB system, referred to as IUWB is considered. The phase shifting at the IRS panel is set by considering the strongest path optimization (SPO) of UWB channel. The SPO has a very close performance to the CPS. However, the CPS is impractical in UWB systems due to the frequency selective channel. The BER and sum-rate performance of IUWB are analyzed. The performance of IUWB improves with an increase in the number of reflecting elements at the IRS. The study also investigates the impact of different UWB channel models (such as IEEE 802.15.4a CM1, CM2, etc.), the number of reflecting elements , phase settings at the IRS, and the IRS position between the BS and UE. The effects of imperfect channel state information are also considered in IUWB. Furthermore, the coverage probability and energy efficiency of IUWB are analyzed. Simulation results demonstrate a significant improvement in

[1]Low SNR scenarios are vital as they challenge the development of robust signal processing techniques essential for reliable communication, accurate data analysis, and improved signal detection.

UWB performance when IRS is employed compared to conventional UWB systems without IRS.

6.2 Proposed IRS-UWB System Model

In this section, the proposed IUWB system model is described, where both the BS and the UE have a single antenna, as shown in Figure 6.1. The UE receives information through both BS-IRS-UE and BS-UE links. Further, the UE uses a Rake structure to resolve the UWB channel paths [49]. Let L_0 be the number of delayed taps in the BS-UE direct channel link; L_1 and L_2 denote taps in the BS-IRS and IRS-UE channel links, respectively. The channel $\mathbf{h}^d = [h_0^d, h_1^d, \cdots, h_{L_0-1}^d]^T$ represents the BS-UE UWB channel link. Similarly, $\mathbf{h}_n^{bi} = [h_{n0}^{bi}, h_{n1}^{bi}, \cdots, h_{n(L_1-1)}^{bi}]^T$ and $\mathbf{h}_n^{iu} = [h_{n0}^{iu}, h_{n1}^{iu}, \cdots, h_{n(L_2-1)}^{iu}]^T$ are the BS-IRS and IRS-UE UWB channel taps in the time-domain, respectively for the nth IRS reflecting element.

Transmitted UWB signal for a single frame is expressed as [126]

$$x(t) = \sum_{i=0}^{N_s-1} d\sqrt{E_\mathrm{b}} w(t - c_i T_c - jT_f), \tag{6.1}$$

where $w(t)$ is unit energy transmitted waveform of time duration T_w sec. E_b denotes the energy of transmit signal for the data symbol $d \in \{-1, 1\}$. The c_i and T_c represent the time hopping code of length N_s and chip duration, respectively with $N_\mathrm{s}T_\mathrm{c} < T_\mathrm{f}$ [127] and T_f is the frame duration.

The impinged signal on the n^{th} IRS element is given as

$$y_{n,\mathrm{irs}}(t) = \sum_{l=0}^{L_1-1} h_{nl}^{bi} x(t - \tau_l(t)), \tag{6.2}$$

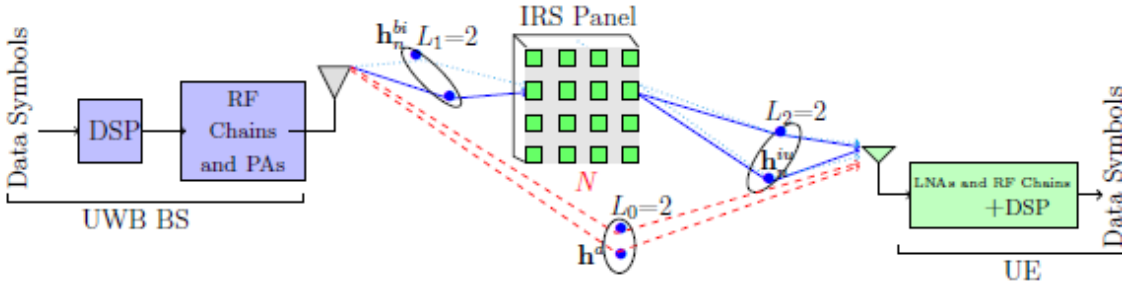

FIGURE 6.1: Proposed IUWB system model. Only 2 channel taps in all the three channels are depicted.

where h_{nl}^{bi} and $\tau_l(t)$ denote the l^{th} $(l = 0, 1, \cdots, L_1 - 1)$ path channel coefficient and delay, respectively. The reflected signal by the nth IRS element is expressed as

$$\begin{aligned} y_n(t, \text{out}) &= \beta_n y_{n,\text{irs}}(t - t_n) \\ &\approx \beta_n e^{j\theta_n} \left[\sum_{l=0}^{L_1-1} h_{nl}^{bi} x(t - \tau_l(t)) \right], \end{aligned} \tag{6.3}$$

where t_n is the time delay of the nth element. The $\theta_n = 2\pi - 2\pi f t_n$ denotes the phase shift at nth element of IRS with signal frequency f (Hertz), and β_n denotes the reflection coefficient of n IRS element. The received signal at the UE via nth IRS element is expressed as

$$\begin{aligned} y_n(t) &= \sum_{l'=0}^{L_2-1} h_{nl'}^{iu} y_n(t - \tau_{l'(t)}) \\ &= \sum_{l'=0}^{L_2-1} h_{nl'}^{iu} \beta_n e^{j\theta_n} \left[\sum_{l=0}^{L_1-1} h_{nl}^{bi} x(t - \tau_l(t) - \tau_{l'}(t)) \right] \\ &= \beta_n e^{j\theta_n} \left[\sum_{l=1}^{L_1-1} \sum_{l'=0}^{L_2-1} h_{ll'}^{n} x(t - \tau_{ll'}(t)) \right], \end{aligned} \tag{6.4}$$

where effective channel coefficient is $h_{ll'}^n = h_{nl'}^{iu} h_{nl}^{bi}$ and the effective delay is $\tau_{ll'}(t) = \tau_{l'}(t) + \tau_l(t)$ of a cascaded path (BS-IRS-UE) for nth IRS element. Therefore, $L_1 L_2$ paths exist in the cascaded channel between BS and UE. Let N be the total reflecting

elements at the IRS panel. The received signal at the UE is

$$r_c(t) = \sum_{n=1}^{N} y_n(t) = \sum_{n=1}^{N} \beta_n e^{j\theta_n} \left[\sum_{l=0}^{L_1-1} \sum_{l'=0}^{L_2-1} h_{ll'}^n x(t - \tau_{ll'}(t)) \right]. \tag{6.5}$$

Further, the received signal $r_d(t)$ at the user through a direct link is given by

$$r_d(t) = \sum_{m=0}^{L_0-1} h_m^d x(t - \tau_m(t)), \tag{6.6}$$

where h_m and τ_m denote the direct path coefficient and delay respectively. The composite received signal $r(t)$ through both the direct and IRS reflected channels is expressed as

$$\begin{aligned} r(t) &= r_d(t) + r_c(t) + n(t) \\ &= \sum_{m=0}^{L_0-1} h_m^d x(t - \tau_m(t)) + \sum_{n=1}^{N} \beta_n e^{j\theta_n} \times \\ &\quad \left[\sum_{l=0}^{L_1-1} \sum_{l'=0}^{L_2-1} h_{ll'}^n x(t - \tau_{ll'}(t)) \right] + n(t) \\ &= h(t) \star x(t) + n(t), \end{aligned} \tag{6.7}$$

where $\star$ denotes the convolution operator, and $h(t)$ is the composite effective channel impulse response (CIR) at the UE as

$$h(t) = \sum_{m=0}^{L_0-1} h_m^d \delta(t - \tau_m) + \sum_{n=1}^{N} \beta_n e^{j\theta_n} \left[\sum_{l=0}^{L_1 L_2-1} h_l^n \delta(t - \tau_l(t)) \right]. \tag{6.8}$$

Therefore, the maximum delay spread of $h(t)$ determines by the number of taps in the cascaded channel. Performance of IUWB depends on the phase of the IRS panel and it can be optimized by maximizing the received signal energy at the UE.

The normalized SNR using three phase settings of RIS elements is shown in Figure

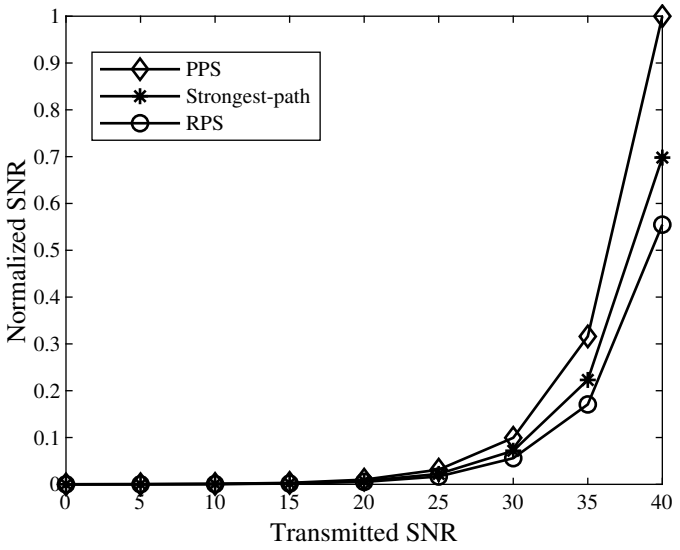

FIGURE 6.2: Normalized SNR plot by considering PPS, RPS, and strongest-path methods at the RIS panel for $N = 2$.

6.2. Perfect phase shift (PPS)[2] gives the best SNR. However, PPS is not practically viable in the multipath scenario. Strongest-path yields higher SNR than the random phase shift (RPS). Henceforth, we consider only PPS and RPS methods only for simplicity.

6.3 Reflection Optimization

In this section, a reflection of impinged UWB signal is optimized to enhance the system performance since the performance of IRS-assisted system depends on the phase of IRS panel. The phase shift matrix $\mathbf{\Theta} = \text{diag}[\beta_1 e^{j\theta_1}, \beta_1 e^{j\theta_1}, \cdots \beta_N e^{j\theta_N}]$ is optimized such that the SNR is enhanced at the UE. The $\beta_n \leq 1$ and $\theta_n, n = 1, \cdots, N$ denotes reflection and phase of the nth element. The phase optimization

[2]Also known as CPS

problem can be expressed as

$$\boldsymbol{\Theta}_{\text{Opt}} = \max_{\boldsymbol{\Theta}\in[0,2\pi)} \zeta_s, \tag{6.9}$$

$$\zeta_s = || \sum_{m=0}^{L_0-1} h_m^d \delta(t-\tau_m) + \sum_{n=1}^{N} \beta_n e^{j\theta_n} \left[\sum_{l=0}^{L_1 L_2 - 1} h_l^n \delta(t-\tau_l(t)) \right] ||^2$$

Phase optimization is done such that the received signal strength is maximum. Performance of IUWB depends on the choice of phase θ_n $\forall n$ as shown in (6.9). We consider three different phase shift methods as: a) Random phase shift (RPS), b) CPS, and c) SPO. In RPS, phase of reflecting elements is randomly selected between 0 and 2π. Therefore, the CIR information is not required at the IRS panel, and RPS has the lowest complexity. However, the reflected signal may not result in a constructive superposition of signal at the UE. In CPS, the perfect phase cancellation among all the paths is considered, and the reflected signal is perfectly aligned towards the UE. Therefore, effectively received signal using absolute value of channel taps is expressed as

$$\sum_{m=0}^{L_0-1} h_m^d \delta(t-\tau_m) + \sum_{n=1}^{N} \beta_n e^{j\theta_n} \left[\sum_{l=0}^{L_1 L_2 - 1} |h_l^n| \delta(t-\tau_l(t)) \right].$$

Therefore, for perfect phase cancellation, phase of each element is set as

$$\theta_n + \angle h_1^n = \theta_n + \angle h_2^n = ..., = \theta_n + \angle h_{L_1 L_2 - 1}^n = 0.$$

Hence, θ_n does not have a unique solution and the CPS at the IRS panel is not possible in practice. Therefore, θ_n can be optimized using the strongest path of the CIR. UWB CIR contains numerous taps, making it impractical to achieve perfect phase cancellation at the IRS. Therefore, we seek to find a θ_n using the strongest path of CIR, and we show through simulations that this approach achieve a performance

close to CPS. The strongest path gain is selected as

$$l^{\star} = \arg \max_{l=1,\ldots,L_1 L_2} \left| \left(h_l^d + \sum_{n=1}^{N} \beta_n e^{j\theta_n} h_l^n \right) \right|^2 . \tag{6.10}$$

Considering only the non-zero channel taps in the cascaded and direct channels, $l^{\star}$ is calculated. Once the strongest path of CIR is estimated, then the IRS phase factors are aligned to the strongest path direction to optimize the channel gain at the UE. Further, other paths apart from the strongest path may also have the same phase as the strongest path. Hence, effective channel gain at the UE comes from the multipath along with the maximum path. The IRS phase using SPO is given as

$$\theta_n = -\angle h_{l^{\star}}^d + \angle h_{l^{\star}}^n, \ n = 1, \cdots, N. \tag{6.11}$$

Furthermore, energy of UWB CIR is not uniformly distributed within a frame [49], therefore, the finding of $l^{\star}$ is much simpler.

6.3.1 Signal Detection

UE performs the equalization to decode the information symbols. UE receives the signal from both the direct link and the BS-IRS-UE link. Coherent detection [126] is used to decode the transmitted data symbols. The detector output for a single frame is expressed as

$$r = d\sqrt{E_{\mathrm{b}}} \left[\sum_{m=0}^{L_0-1} (|h_m^d|)^2 + \sum_{n=1}^{N} \sum_{l=0}^{L_1 L_2 - 1} (|h_l^n|)^2 \right] + N_n, \tag{6.12}$$

where N_n is the filtered zero-mean Gaussian noise with variance $\sigma_{N_n}^2$. In (6.12), we assume unit energy Gaussian pulse and the reference signal is generated by considering perfect knowledge of channel state information [50]. The detector output

is passed through a threshold circuit with zero threshold by considering both symbols are equally likely.

Therefore, r is normally distributed as $r \sim \mathcal{N}\left(\sqrt{E_\mathrm{b}}A_s, \sigma^2_{N_n}A_s\right)$,
where $A_s = \left[\sum_{m=0}^{L_0-1}(h_m^d)^2 + \sum_{n=1}^{N}\sum_{l=0}^{L_1L_2-1}(h_l^n)^2\right]$. Hence, the BER $P(e|h(t))$ for given channel is expressed as

$$P(e|h(t)) = Q\left(\frac{\sqrt{E_\mathrm{b}}A_s}{\sqrt{\sigma^2_{N_n}A_s}}\right), \tag{6.13}$$

where $Q(x) = 1/\sqrt{2\pi}\int_x^\infty \exp(-t^2/2)dt$ is the Q-function. Average BER is calculated by averaging $P(e|h(t))$ over all fading coefficients using Monte Carlo simulations.

6.4 Simulations and Discussion

In this section, simulation results demonstrate the effectiveness of the IUWB system for the IEEE 802.15.4a channel models [128]. We consider system bandwidth (BW) is 1 GHz and the reference channel power gain as -30 dB at distance 1m. The UWB pulse energy is set to unity. The path loss exponents are set $\alpha_1 = 2.4$, $\alpha_2 = 2.2$ and $\alpha_3 = 2.1$ for BS-UE, BS-IRS, and IRS-UE links, respectively.

Average BER performance of IUWB is shown in Figure 6.3 for various number of reflecting elements N. As N increases, BER performance improves, as shown in Figure 6.3 due to the increased received signal strength. For example, $N = 64$ SNR gain is around 6 dB at BER $= 10^{-5}$ as compared to $N = 16$, as observed in Figure 6.3. The proposed SPO method (dotted lines) has close performance to the CPS[3] method (solid lines), as observed in Figure 6.3. Further, we also observe (Figure

[3]It is considered solely to demonstrate the upper limit of performance in the IRS UWB system.

6.3) that the diversity also improves as N increases. The RPS method has degraded performance as compared to the proposed SPO and the CPS methods, as shown in Figure 6.3. Semi-analytical (dash-dotted lines) results are matched with simulations, as observed in Figure 6.3.

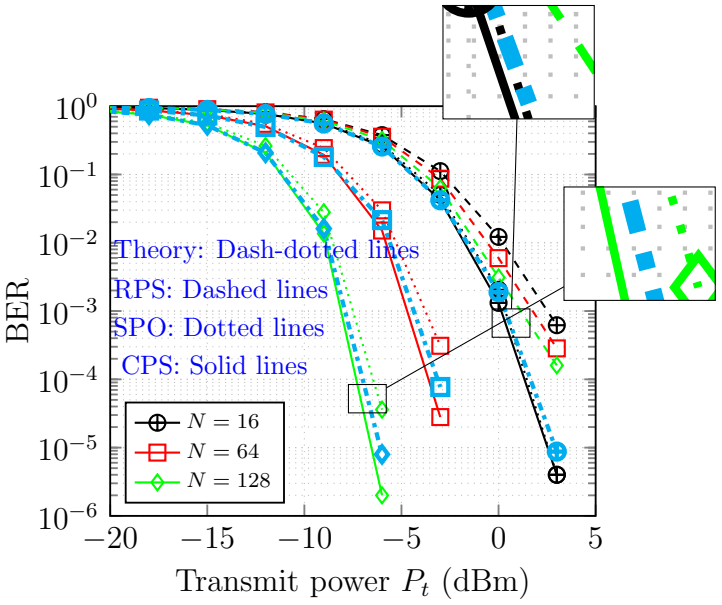

FIGURE 6.3: Average BER of IUWB for $N = 16, 64, 128$ over IEEE 802.15.4a CM1 channel.

Further, the average BER performance of a conventional UWB [127] and the proposed IUWB with both the BS-IRS-UE and BS-UE links is compared in Figure 6.4. For small $N = 16$, the IUWB performance is inferior as compared to the conventional UWB system. However, as N increases, IUWB's BER improves and is better than the conventional UWB [127], as observed in Figure 6.4 due to passive beamforming at the IRS, which results in SNR enhancement at the UE.

Impact of the location of IRS panel: Impact of RIS location on BER performance is shown in Figure 6.5 by considering the fixed transmitted power $P_t = 0$ dBm. In Figure 6.5, only BS-IRS-UE link exists and the direct link (BS-UE) is blocked in IUWB and the distance between BS and UE is 100m. We observe that if IRS panel is near to BS or user gives lower BER performance as compared to

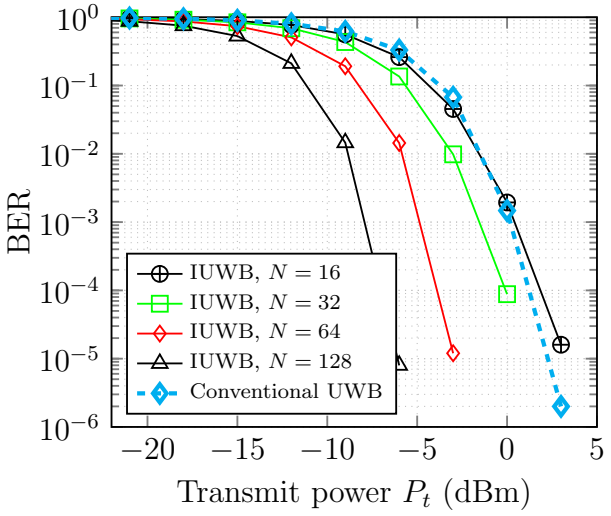

FIGURE 6.4: BER performance of IUWB and conventional UWB without IRS.

other locations of IRS, as observed in Figure 6.5 due to lower pathloss of the cascaded channel. Further, we observe that the higher N results in improved BER performance for all the positions of IRS.

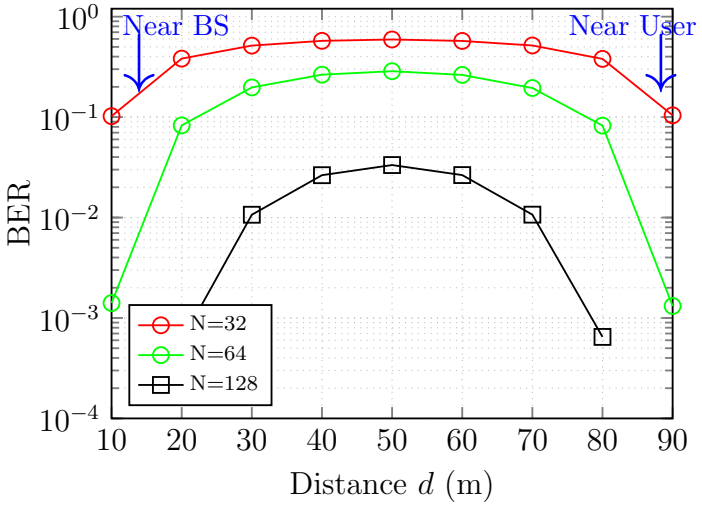

FIGURE 6.5: BER performance of IUWB based on IRS position.

Sum-rate analysis: Average sum-rate performance of IUWB system is shown in Figure 6.6 for a different number of reflecting elements N by considering $\log_2(1 + \text{SNR})$ bps/Hz. As N increases, the sum-rate improves, as observed in Figure 6.6 due

to the enhancement of the signal amplitude. We consider both direct (BS-UE) plus BS-IRS-UE links (DIRSL) and only BS-IRS-UE link (IRSL) in Figure 6.6. DIRSL gives better sum-rate performance (around 1 bps/Hz gain at P_t=10dBm for $N = 16$) as compared to the IRSL for smaller values of N, as observed in Figure 6.6. However, both DIRSL and IRSL have very close performance for $N = 128$ since direct link does not have any significant contribution to the proposed IUWB system for a larger value of N. Further, the sum-rate of a conventional UWB (without IRS) [48] is lower than the IUWB system, as observed in Figure 6.6. Hence, a non-zero sum-rate is achieved at low SNR region by choosing a higher value of N.

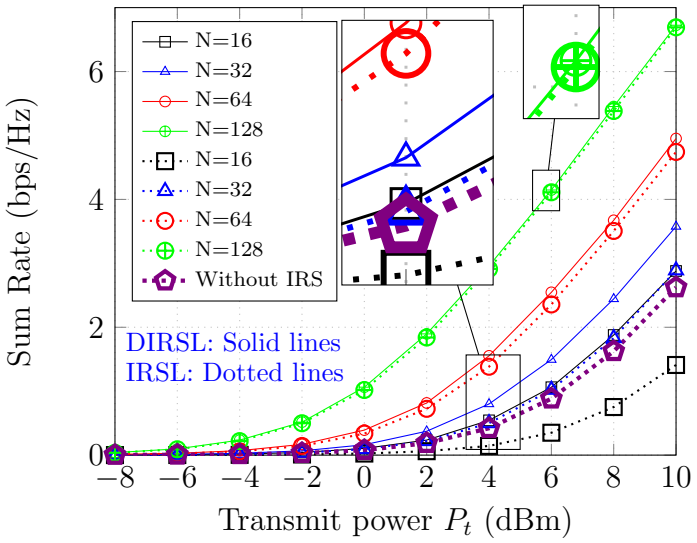

FIGURE 6.6: The sum-rate vs SNR performance of IUWB system over IEEE 802.15.4a CM1 channel.

Imperfect CIR: The estimated CIR with imperfect CIR $\hat{\mathbf{h}}$ can be modeled as [129]

$$\hat{\mathbf{h}} = \sqrt{\rho}\mathbf{h} + \sqrt{(1-\rho)}\mathbf{e}, \tag{6.14}$$

where $\mathbf{h}$ is the actual CIR, $\rho \in [0, 1]$ is the CIR accuracy parameter and $\mathbf{e}$ is an error vector with entries following an i.i.d. $\mathcal{CN}(0, \sigma_h^2)$. σ_h^2 denotes the channel variance. BER degrades in imperfect CIR cases as compared to perfect CIR, as shown in Figure

6.7. Further, a larger estimation error leads to severe BER degradation, as observed in Figure 6.7. due to larger residual interference. This observation demonstrates that perfect CIR is a prerequisite to unlock the full potential of IRS beamforming in IUWB.

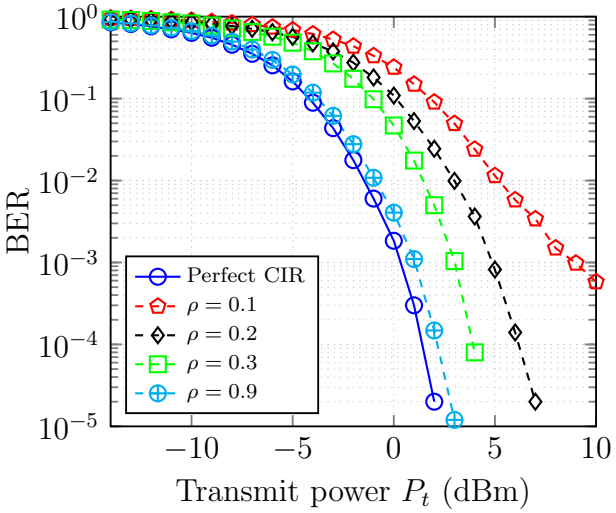

FIGURE 6.7: Average BER of IUWB for N=16 over IEEE 802.15.4a CM1 channel.

Coverage probability: Coverage probability is defined as the probability when the effective received SNR at the UE is larger than a given threshold γ_{thr}. Therefore, coverage probability is defined as $P(\text{SNR} \geq \gamma_{\text{thr}})$. Average coverage probability analysis of the IUWB system is shown in Figure 6.8 with conventional UWB system without IRS. We consider $\gamma_{\text{thr}} = 20dBm$ and the number of reflecting elements varies in Figure 6.8. The IUWB enhances the coverage probability over conventional UWB system, as observed in Figure 6.8 due to higher received signal strength. Further, the coverage probability of IUWB improves as the number of reflecting elements increases.

Energy Efficiency: Energy efficiency (EE) of IUWB system is calculated using the sum-rate and power consumption of IUWB. The total power consumption of IUWB

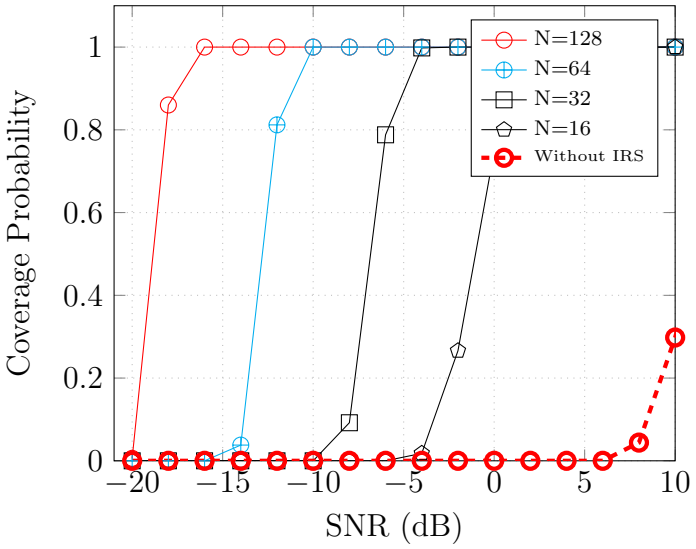

FIGURE 6.8: Coverage probability versus SNR analysis of IUWB.

is defined as

$$P_{\text{tot}} = \nu P_{\text{t}} + P_{\text{s}} + P_{\text{r}} + N \times P_{\text{n}},$$

where ν and P_{t} denote the power amplifier efficiency and transmit power, respectively. P_{s} and P_{r} are the power consumption at the transmitter and receiver, respectively, and P_{n} is dissipated power at each IRS element. Figure 6.9 shows the EE as a function of SNR of the IUWB system. We consider $\nu = 0.5$, $P_{\text{t}} = 1$ W, $P_{\text{s}} = 100$ mW, $P_{\text{r}} = 100$ mW, and $P_{\text{n}} = 5$ mW for both IUWB and conventional UWB without IRS. The energy efficiency of IUWB outperforms the conventional UWB without IRS, as observed in Figure 6.9 for all the values of N. Further, it is observed that the energy efficiency of IUWB at high SNR is the same for $N = 32$ and $N = 64$. Since more elements at the IRS panel results in higher power dissipation.

Time-of-arrival (ToA) performance of the IUWB is analyzed by considering the maximum energy path in the received signal [130]. The received signal within a frame is divided into five smaller sub-intervals. Then, the maximum energy sub-interval is selected for ToA estimation. The ToA error is calculated between the actual maximum energy path index and the received signal of maximum energy

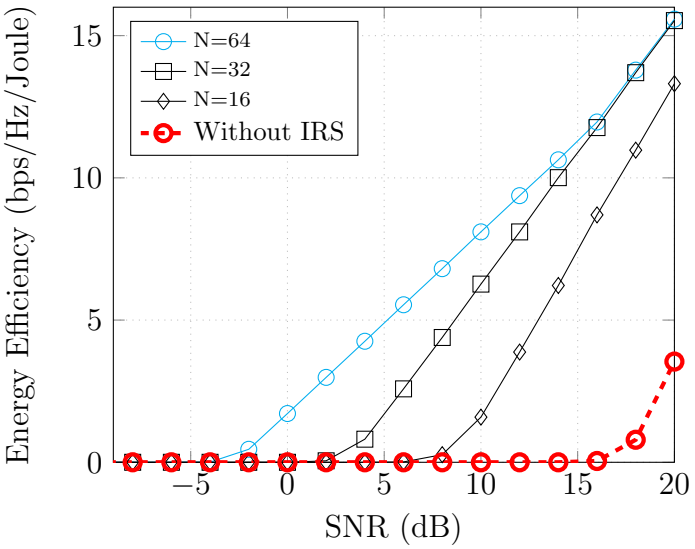

FIGURE 6.9: Average energy efficiency of IUWB system by varying number of reflecting elements.

sub-interval as in [130]. The ToA performance with different SNR is plotted in Figure 6.10. The sampling frequency is 9 GHz and a sub-interval time duration is 10 ns in Figure 6.10. As N increases, ToA accuracy improves for both PPS (solid lines) and RPS (dashed lines) scenarios, as observed in Figure 6.10. Further, the ToA performance of conventional UWB without RIS (Without RIS) is also plotted in Figure 6.10 for comparison. The IUWB gives better ToA accuracy as compared to conventional UWB system [22] due to higher received signal strength.

6.5 Summary

The proposed IUWB system utilizes an IRS for energy-efficient system design. The analysis focuses on the BER and sum-rate performance of IUWB. A novel phase optimization method based on the strongest path is proposed and compared with coherent and random phase shift methods. Results show that the proposed strongest path-based phase method exhibits similar BER performance to the coherent phase

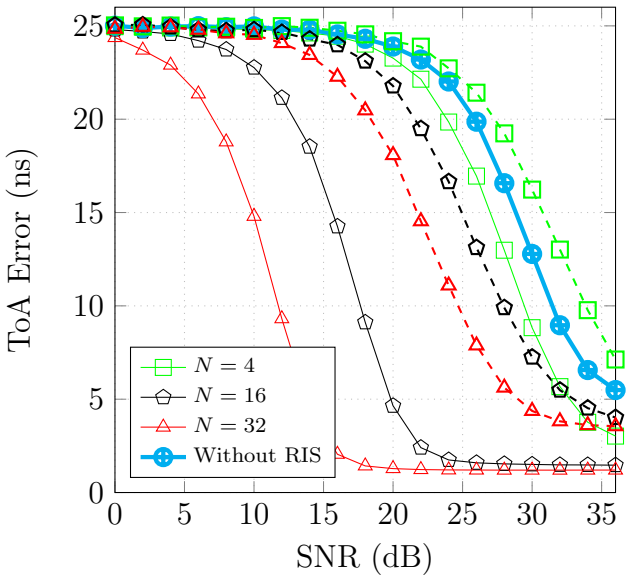

FIGURE 6.10: Average ToA performance of IUWB. Solid and dashed lines denote the PPS and RPS performance, respectively.

method. The impact of different UWB channels and the number of reflecting elements on IUWB performance is studied and compared with a conventional UWB system without IRS. The findings indicate that increasing the number of reflecting elements improves the sum-rate and BER performance of IUWB. Additionally, the positioning of the IRS near the BS or UE yields better performance compared to other positions. Future research directions may include the analysis of joint localization and communication for IUWB in indoor scenarios. Moreover, considering IRS-related channel estimation with multipath is challenging due to the limited signal processing capability of the IRS.